International Journal of Computational and Theoretical Chemistry
2025, Vol. 13, No. 1, pp. 25-42
https://doi.org/10.11648/j.ijctc.20251301.13

Research Article

DFT Study on Potassium Benzene Disulfonamide and Potassium Phthalimide Ionic Liquid Based Carbon Dioxide Absorption

Berihun Tibebu[1, *], Abdudin Geremu[2], Endale Tsegaye[2]

[1]Department of Chemistry, Jinka University, Jinka, Ethiopia
[2]Department of Chemistry, Hawassa University, Hawassa, Ethiopia

Abstract

This groundbreaking research rigorously investigated the CO_2 absorption potential of two potassium-based ionic liquids (ILs), namely potassium benzene disulfonamide [$C_6H_4KNS_2O_4$] and potassium phthalimide [$C_8H_4KNO_2$]. Driven by the urgent need for effective carbon capture technologies to combat climate change stemming from fossil fuel combustion, this study employed sophisticated Density Functional Theory (DFT) calculations using the M062X/6-31+G(d,p) method. The computational approach encompassed comprehensive geometry optimization, in-depth molecular interaction analyses, precise binding energy assessments, insightful Natural Bond Orbital (NBO) analysis, and a thorough evaluation of solvent effects. The findings unequivocally demonstrate that both ILs exhibit tangible interactions with CO_2, with binding energies ranging from -3.108 to -0.232 kcal/mol for $C_6H_4KNS_2O_4$ and -3.475 to -0.219 kcal/mol for $C_8H_4KNO_2$. These energies strongly suggest the viability of these ILs for CO_2 capture applications, potentially requiring minimal energy for regeneration. Crucially, the research established that potassium benzene disulfonamide [$C_6H_4KNS_2O_4$] displays superior CO_2 capture efficacy compared to potassium phthalimide [$C_8H_4KNO_2$]**.** This conclusion is robustly supported by compelling thermochemical and molecular interaction data. NBO analysis further elucidated that CO_2 interaction induces alterations in the IL geometry and facilitates charge transfer between the interacting species. Moreover, studies on cation-anion interactions revealed a stronger association between $C_6H_4KNS_2O_4$ and the potassium cation (K^+). Investigation of isolated anion interactions with CO_2 echoed the preference for [$C_6H_4NS_2O_4$]. While solvent effects influenced thermochemical properties, they did not fundamentally alter the geometry of the anion-CO_2 complexes. In conclusion, the computational evidence unequivocally indicates the formation of stable complexes between the investigated IL pairs and CO_2 molecules. Most significantly, this study firmly establishes that $C_6H_4KNS_2O_4$ is a more promising candidate for efficient CO_2 absorption**,** offering a pathway towards the development of advanced and effective CO_2 capture technologies.

Keywords

Absorption, Binding Energy, Carbon Dioxide, DFT, Ionic LIquid, NBO Analysis

*Corresponding author: berihuntibebu16@gmail.com (Berihun Tibebu)

Received: 9 January 2025; **Accepted:** 19 July 2025; **Published:** 10 April 2025

1. Introduction

CO_2 is one of the major greenhouse gases in the quantum world that cause significant effects on climate change [1]. The burning of fossil fuels to produce electricity and heat empowered the release of large quantities of CO_2 into the atmosphere. In recent years, CO_2 has been found to be a major contributor and one of the most challenging environmental issues facing worldwide climate change [2]. This has inspired researchers in the area of CO_2 capture strategy advancement. Gür T. M. [3] Studied quite a lot of readily ac

cessible CO_2 capture strategies through an absorption technology, which could be used to alleviate CO_2 emissions. One of the key significances under development is a new, faster, high absorption rate for CO_2 and good chemical stability. Much research has been devoted to finding or designing new solvents or materials for CO_2 separation through chemical/physical absorption, chemical/physical adsorption, membranes, solid adsorbents, and biomimetic approaches [4]. There are different technologies for CO_2 capture in the world, although they are energy intensive, far from cost-effective, and not attractive for large-scale applications [1].

The recent comprehensive review on high- temperature energy cells with carbon internee studies [5] indicate that the CO_2 internee strategy enhancement will continue competitively in the future because CO_2 emigrations is adding due to increase in energy demands for the growing artificial revolution. The discoveries and uses of special classes of ILs as absorption paraphernalia took place a long time a gone until the late 1990s, in the areas of electrochemistry and organic chemistry. These have been changed suddenly as a result of an composition published by Freemantle [6] in 1998 that reported the implicit operations of ILs as a new soap for green chemistry [7] also, the tunability parcels of ILs give an spare degree of freedom for designing cleansers with certain specific characteristics [8]. This prolusion provides a suggestion on the scale of the problem and the resolution to take action in order to help unrecoverable climate change. It was first reported by Blanchard et al., 1999 [9] that sizable amounts of CO_2 might dissolve in imidazolium-ground ILs to facilitate the formation of a dissolved product. This work sparked a flurry of scientific research on the topic of CO_2 immersion with ILs, which quickly expanded the body of knowledge on this particular topic [8].

At the moment, monoethanol amine (MEA) is still thought to be the primary detergent in waterless alkanol amine-grounded prisoner process outcomes. due to its many benefits over other commercially available alkanolamines, such as its low molecular weight, strong reactivity, and inexpensive solvent cost. Therefore, a high absorbing capacity on a mass base, reasonable thermal stability, and thermal declination rate [10]. The disadvantages of MEA include the high enthalpy of response with CO_2 leading to a high energy demand due to the conformation of a stable carbamate and also the conformation of declination products with oxygen-containing feasts. Furthermore, amine-ground detergents' inability to eliminate mercaptans, high vapor pressure-induced vaporization losses, and superior cattiness compared to several other alkanolamines [11] suggest the necessity for an essential detergent system.

MEA is a basic instance in this field because of its broad application and benefits over other alkanolamines; nonetheless, the anticipated shortcomings of this amine-based solvent prompt the scientific community to discover additional essential detergents for CO_2 immersion. CO_2 prisoner by ILs has been presented as an implicit volition system due of its unique properties. ILs, which are organic mariners that live as liquids under room temperature and which are polar detergents with no vapor pressure, non-flammability, high thermal stability, fairly low density, wide temperature ranges for big liquids, high ionic conductivity, and nonvolatile material, have been considered for numerous operations [12]. Thus, this work is intended to hunt for a suitable IL for CO_2 prisoner from stove pipe- gas aqueducts and other point sources and probe computationally using the Density functional study (DFT) system to understand the medium of the immersion process. This is one of the possible approaches that can be used to ameliorate CO_2 prisoner technology.

2. Computational Detail

The Gaussian 09 software program was used to execute all quantum chemical calculations, whereas Gauss View 5.0.9 [13] was used to build all inputs for this investigation. First, the PM6 [14] model was used to perform semi-empirical computations to identify the most stable structures among all inputs. All computations were performed using the DFT [15] technique with no symmetry restrictions, using the 631+G(d,p) basis set [16] and the M062X [17] functional. By calculating frequency, each optimized structure was verified to be a real minimum. The absence of imaginary frequency in the ground state optimized structures confirms that they coincide with potential energy surface minima [18]. Vibrational frequency calculations have been used to get the thermochemical data for the partnering interactions of carbon dioxide with anions and ILs under standard conditions. This document reports all energies with thermal energy correction and zero point energy included. The presented thermochemical results were not corrected for basis set superposition errors. The binding energy, ΔB.E, which is the energy difference between the complex's total energy and the energy sum of each monomer that makes up the complex using equations (1), and the enthalpy of interaction, ΔH, were calculated using equations (2) [19]. Using the associated equation (3) [19], the additional thermodynamic parameters, such as the change in entropies, ΔS, were computed.

$$\Delta B.E = B.EIL - CO_2 - (B.EIL + B.ECO_2) \quad (1)$$

$$\Delta H = HIL - CO_2 - (HIL + HCO_2) \quad (2)$$

$$\Delta S = SIL\text{-}CO_2\text{-}(SIL+SCO_2) \quad (3)$$

NBO analysis [20] and electrostatic implicit analysis have also been performed at the M062X/ 6- 31 G(d, p) position to gain a deeper appreciation of the nature of the relations between ionic ILs and their complexes with CO_2. Natural bond orbital studies have a resource-full system to anatomize intramolecular and intermolecular relations. NBO analysis stresses the part of intermolecular orbital commerce in the complex, particularly charge transfer. This is carried out by considering all possible relations between filled patron and empty acceptor NBOs and estimating their energetic significance using alternate order anxiety proposition [21]. For each patron NBO (i) and acceptor NBO(j), the stabilization energy, $E^{(2)}$ equation (4) associated with electron delocalization between patron and acceptor is estimated as follow.

$$E^{(2)} = q_i \frac{F(i,j)^2}{\varepsilon_j - \varepsilon_i} \quad (4)$$

Where q_i is the orbital occupancy, ε_i, ε_j are diagonal elements and $F_{i,j}$ is the off-diagonal NBO Fock matrix elements.

The solvent effect has been implicitly calculated using the self-consistent reaction field (SCRF) method using the polarizable continuum model (PCM) created by Dhar and Fahim's group [22] for the polar protic (water) and polar aprotic (chloroform and DMSO) solvents in order to reduce the unrealistic effect of this computational investigation. The M062X functional [23], which can predict interaction energies in greater agreement with experimental data than the B3LYP functional [24], was used to calculate all inputs for this computational investigation in gases and solvents.

3. Results and Discussions

3.1. Structural Features of CO_2 and Anions

CO_2 is a carbon conflation in which the carbon is connected covalently to each oxygen grain by a double bond. CO_2 is a white odorless gas at room temperature and pressure. In order to determine the commerce point, the frontier molecular orbitals (HOMO and LUMO) and molecular electrostatic eventuality (MESP) map of CO_2 were analyzed as depicted in Figure 1. The HOMO of CO_2 concentrated over O- particles, and the LUMO of CO_2 concentrated over C- particles. The ESP map of the CO_2 patch shows that the O- particles bear negative charges and the C- particles bear positive charges. Therefore, the frontier molecular orbital analysis and ESP map visualization indicate that the C- grain of CO_2 is read for electrophilic commerce, whereas O- particles are read for nucleophilic commerce. CO_2 is nonpolar and contains two polar bonds that are arranged symmetrically and cancel each other. The dipole moment of CO_2 is zero. The optimized structure of CO_2 patch at M062X/6-31G(d,p) position in gas phase gives its geometric parameters, analogous as the bond angle between (O-C-O) is 180^0 and the bond length (C- O) of 1.169 Å, which are in good agreement with the experimental values of 180^0 for the angle and 1.163 Å for the bond length [25].

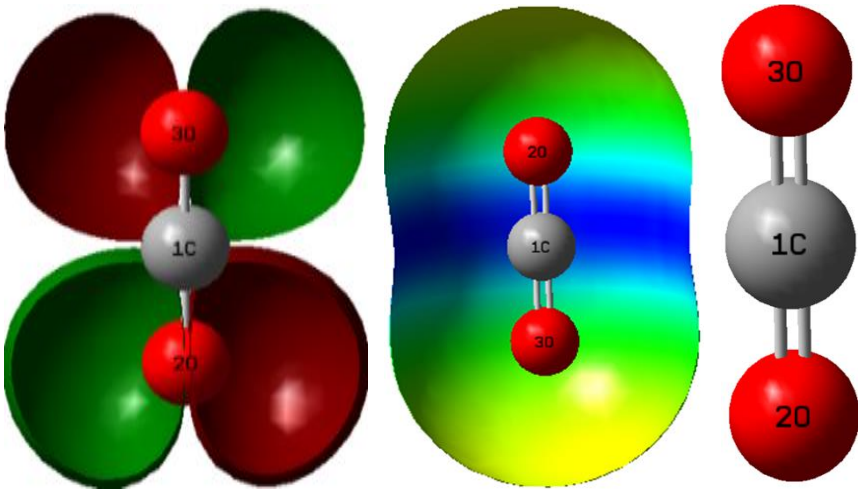

(a) (b) (c)

Figure 1. *(a), HOMO-LUMO, (b) ESP map and (c), Optimized structures of CO_2 calculated at M062X/6-31+G(d,p) level in gas phase.*

The geometries of two anions, $[C_6H_4NS_2O_4]$ and $[C_8H_4NO_2]$, were optimized using the DFT method with the M062X functional and 6-31+G(d.p) basis set, ensuring the absence of imaginary frequencies in their ground states. For the $[C_6H_4NS_2O_4]$ anion, the bond angles between atoms (e.g., O16, S12, O17 = O14, S11, O15 = 115.780 and N13, S11, O14

= N13, S12, O17 = 110.640) reflect interactions within sulfonate and nitrogen-sulfur-oxygen environments. For [$C_8H_4NO_2$], bond angles such as C1, C7, N13 = C2, C8, N13 = 109.690 and N13, C7, O15 = N13, C8, O14 = 128.260 suggest typical aromatic sp^2 hybridization and conjugative interactions between nitrogen, carbon, and oxygen atoms. These angles reveal structural features related to conjugation, electronic interactions, and bond strain in the anions.

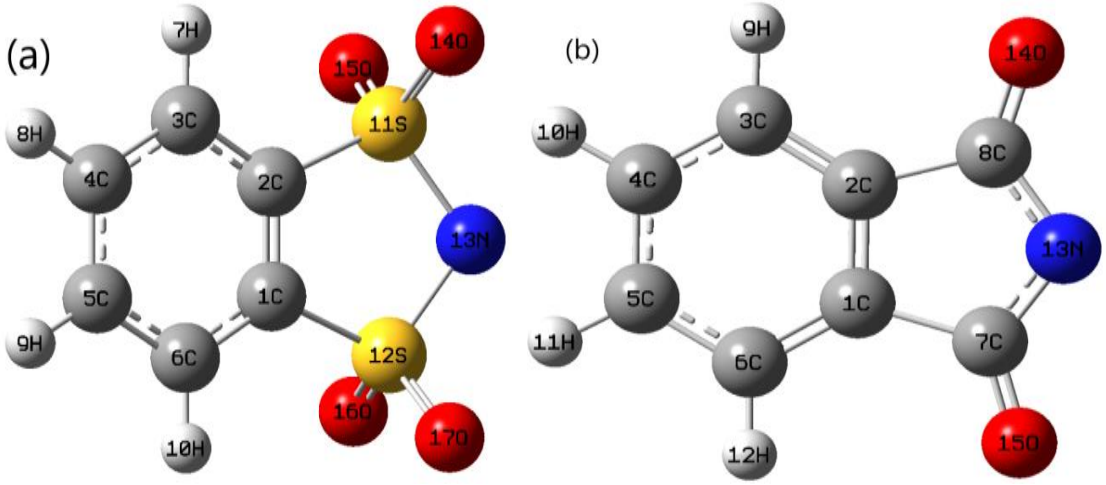

Figure 2. *The geometric parameters for the optimized structures of (a) for [$C_6H_4NS_2O_4$] and (b) for [$C_8H_4NO_2$] anions calculated at M062X/6-31+G(d,p) level in gas phase.*

The electrostatic potential (ESP) map of the anions $C_6H_4KNS_2O_4$ and $C_8H_4KNO_2$, calculated at the M062X/6-31+G(d,p) level, reveals highly negative regions (red areas) concentrated around the oxygen and nitrogen atoms, indicating high electron density. These regions are potential sites for interaction with CO_2, which could be driven by electrostatic forces between the negatively charged anions and the partially positive carbon atom of CO_2. Additionally, the partially yellow areas on the map represent regions where van der Waals interactions may occur, involving weaker attractions between carbon and hydrogen atoms. The electron density redistribution in these anions gives rise to a net negative charge on the oxygen and nitrogen atoms, highlighting multiple possible interaction sites for CO_2.

(a) (b)

Figure 3. *ESP map of (a) for [$C_6H_4NS_2O_4$] and (b) for [$C_8H_4NO_2$] anions calculated at M062X/6-31+G(d,p) level in gas phase.*

3.2. Cation-Anions Interaction of the ILs

To determine stable conformers of the ILs, the geometries of the K^+ ion and the anions ($C_8H_4KNO_2$ and $C_6H_4KNS_2O_4$) were optimized separately at the M062X/6-31+G(d,p) level. The K^+ ion was then positioned around the anion geometries to form ion pairs, with one stable conformer obtained for each IL. Vibrational frequency calculations showed no imaginary frequencies, confirming that the ion pairs are in their ground

states. Electrostatic potential (ESP) maps revealed high electron density around the N and O atoms of the anions, indicating the sites of strongest electrostatic interaction with K^+. The maps also highlighted Van der Waals interactions (yellow regions) between C-H atoms and the electrostatic presence of K^+ (blue regions). These results demonstrate stable ion pair formation through charge transfer and electrostatic forces.

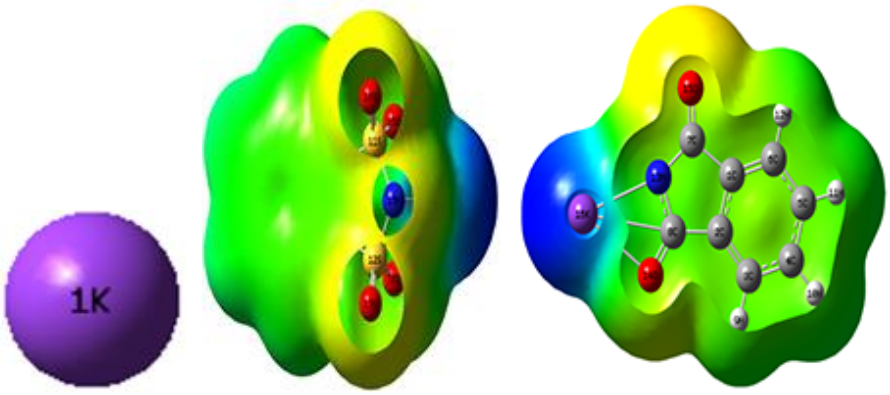

Figure 4. *ESP surface of ILs and the optimized geometry of ion (K^+) calculated at M062X/6-31+G(d,p) level in gas phase.*

The analysis compares the binding energies of two ILs, $C_6H_4KNS_2O_4$ and $C_8H_4KNO_2$, with potassium ions (K^+). The calculated binding energies (ΔB.E) are -127.178 kcal/mol for $C_6H_4KNS_2O_4$ and -115.364 kcal/mol for $C_8H_4KNO_2$, indicating that $C_6H_4KNS_2O_4$ has a stronger interaction with K^+ due to its more negative aspects for binding energy. This suggests that $C_6H_4KNS_2O_4$ is more stable and could be more effective for applications such as CO_2 loading, where strong cation-anion interactions are desirable. From Figure 5, both ILs show direct interactions between K^+ and the N/O atoms of the anions, but the higher binding energy in $C_6H_4KNS_2O_4$ suggests it has a higher potential for CO_2 absorption [26].

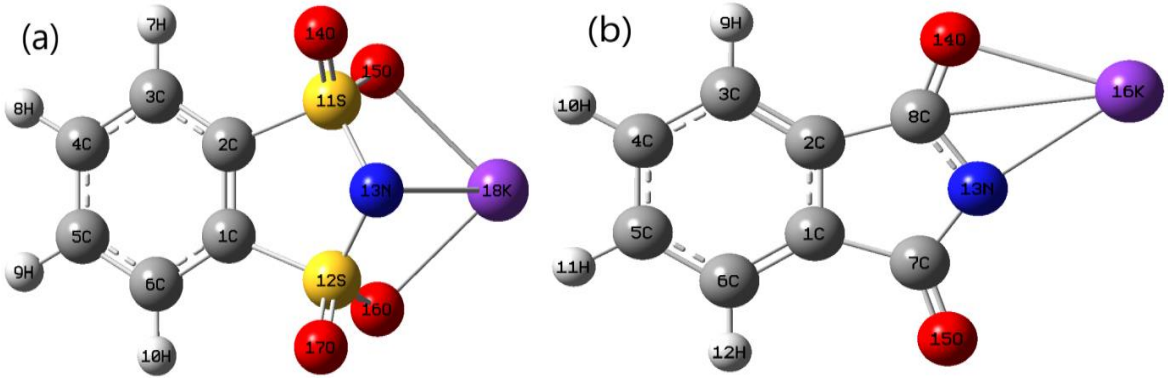

Figure 5. *Ionic pairs comprising a potassium ion, [K^+] with two anion calculated using M062X/6-31+G(d,p) level in gas phase.*

The polarity of the molecule is indicated by its dipole moments and has a significant impact on its interactions with CO_2. The distance between the positive charge center and the negative charge center of an IL pair decreases as the dipole moment decreases. The molecular polarity for the entire IL pair will be stronger if the dipole moments of the ion pairs are larger. Similar rules were observed for ΔB.E. The large negative aspects of the ΔB.E, the stronger the interaction between the cation and anions. Therefore, it is easy to form a coupled structure, which can effectively reduce the interaction between IL pairs, resulting in a low viscosity [12].

Table 1. *Selected thermochemical properties of ion-pairs at M062X/6-31+G(d,p) level in gas phase.*

	Ionic liquids	
Thermochemical data	**$C_6H_4KNS_2O_4$**	**$C_8H_4KNO_2$**
ΔB.E, kcal/ mol	-127.178	-115.364

	Ionic liquids	
Thermochemical data	**$C_6H_4KNS_2O_4$**	**$C_8H_4KNO_2$**
Dipole moment, Debye	7.2959	7.8982

3.3. Interactions of Isolated Anion with CO_2

Schemes 1 and 2 depict the interaction between CO_2 and every selected anion, with the anion's high-electronegative N-atoms being the most strongly bound. The physical and chemical interactions must be consider for the interaction between anion and CO_2: chemisorption of CO_2 come to be about in N-C carbamate bond formation, loss the linearity of the structural model of CO_2, and another structure in which CO_2 is closely physisorbed but no carbamate bond formations occur. This indicates the two C= O bonds in CO_2 bend towards the same direction due to the geometrical position and natural behaviors of O- atoms in both anion and CO_2 molecule. The minimal energy surface [27] was used to observe both soluble ILs and two anions of the chemisorption mechanisms of CO_2 bindings in this progress report.

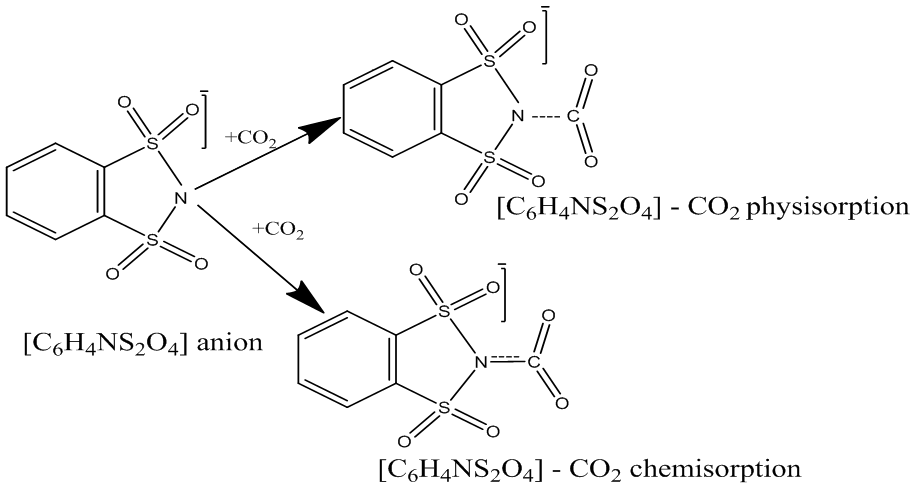

Scheme 1. *Physisorption and Chemisorption mechanisms of $[C_6H_4NS_2O_4]$ - CO_2 from CO_2 and N- interaction, structure of N-heterocyclic $[C_6H_4NS_2O_4]$ - anion.*

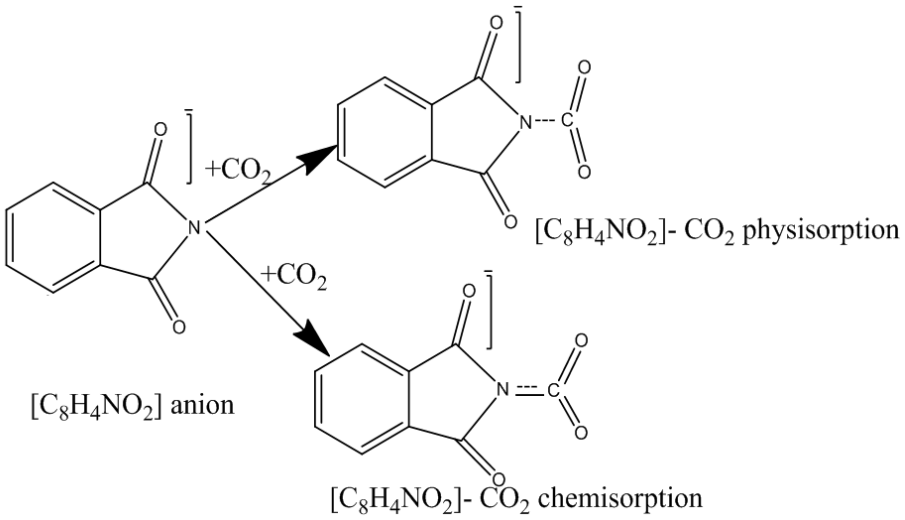

Scheme 2. *The physisorption and chemisorption interaction mechanism between CO_2 and $[C_8H_4NO_2]$ anion.*

The study evaluates the interaction energies (enthalpies, ΔH) between CO_2 and two anions, $[C_6H_4NS_2O_4]$ and $[C_8H_4NO_2]$, across different computational models. The results show that the $[C_6H_4NS_2O_4]$ anion has significantly more negative ΔH values, indicating a stronger and more favorable interaction with CO_2 compared to $[C_8H_4NO_2]$. This stronger

interaction suggests that $[C_6H_4NS_2O_4]$ is more effective for CO_2 absorption, aligning with high experimental CO_2 solubility data from Shifflett and Yokozeki [26]. Thus, $[C_6H_4NS_2O_4]$ is a more suitable candidate for CO_2 capture applications.

The complexes $[C_8H_4NO_2]$ -CO_2 (e) and $[C_8H_4NO_2]$ -CO_2 (g) have strong exothermic interactions with CO_2, making them suitable for CO_2 absorption. The values of these complexes have significantly more negative compared to complex (f), suggesting better CO_2 chemisorption. According to Shifflett and Yokozeki, the high solubility of CO_2 in ions is due to the anion's Lewis basicity, which facilitates charge transfer to CO_2. For the $[C_6H_4NS_2O_4]$-CO_2 complexes, chemisorption energies range from -39.86 to -21.77 kcal/mol, with the most stable configurations showing energies between -39.86 and -37.61 kcal/mol, highlighting their efficiency in CO_2 capture.

The study compares the binding energies and thermodynamic properties of different ion-CO_2 complexes. The $[C_8H_4NO_2]$- CO_2(f) complex is energetically favorable and less energy-demanding for CO_2 capture compared to other complexes like $[C_6H_4NS_2O_4]$ - CO_2, $[C_8H_4NO_2]$- CO_2(e), which require higher energy for chemisorption. Thus, chemical immersion is more suitable for the CO_2 junking process from the stove pipe gas streams or exhaust feasts than physical immersion [28]. The study also shows that $[C_8H_4NO_2]$ and $[C_6H_4KNS_2O_4]$ complexes exhibit strong CO_2 absorption, making them competitive for CO_2 capture. Thermodynamic data, including ΔB.E, ΔH, ΔS, and dipole moment (dpm), are detailed in Table 2 for further analysis.

Table 2. *ΔB.E and ΔH are in kcal/ mol, ΔS in Cal/molk and Dipole moment in Debye of $[C_6H_4NS_2O_4]$ - CO_2 and $[C_8H_4NO_2]$ - CO_2 complexes are presented in the gas phase at M062X/6-31+G (d, p) level.*

(a)	$[C_6H_4NS_2O_4]$-CO_2 complexes	ΔB.E	ΔH	ΔS	Dpm
	$[C_6H_4NS_2O_4]$-CO_2 I (a)	-37.025	-37.61	-28.863	6.42
	$[C_6H_4NS_2O_4]$-CO_2 II (b)	-39.274	-39.86	-30.959	8.86
	$[C_6H_4NS_2O_4]$-CO_2 III (c)	-39.2564	-39.84	-32.124	8.28
	$[C_6H_4NS_2O_4]$-CO_2 IV(d)	-39.26	-39.85	-31.282	8.67
(b)	$[C_8H_4NO_2]$-CO_2 complexes	ΔB.E	ΔH	ΔS	Dpm
	$[C_8H_4NO_2]$-CO_2I (e)	-24.186	-24.77	-32.785	13.26
	$[C_8H_4NO_2]$-CO_2 II (f)	23.336	22.744	-36.702	9.442
	$[C_8H_4NO_2]$-CO_2 III(g)	-21.177	-21.77	-23.228	10.9

The dipole moment in each quantum mechanical computational data analysis for the interactions of anion and ion pairs with CO_2 in the formation of their complexes was one of the significant points to find the different types of stable minimal energy quantum mechanical models between them chemically bonded atoms or molecules [29]. As shown in Figure 3, in the favorable sites, H atoms attack the high electron density atoms of CO_2. The most imaginable sites for nucleophile attack are around H atoms of $[C_6H_4NS_2O_4]$ and $[C_8H_4NO_2]$ anions, which can be visualized clearly. Usually, H-bonds are formed between the high electronegative O atoms of CO_2 and H-atoms of each anion, but their strengths vary and the corresponding optimized models of complexes are stable. With the addition of CO_2 to the $[C_8H_4NO_2]$ ion structure at Figure 6(f), the H- atoms leave the $[C_8H_4NO_2]$ molecule and make a carbamate bond with the C of CO_2. The geometries of anion-CO_2 complexes are shown in Figure 6, in which the strong H- bonds are formed by the shorter bond length between atoms of Hydrogen and Oxygen [30], in $[C_6H_4NS_2O_4]$ -CO_2 and $[C_8H_4NO_2]$ -CO_2 complexes at (b), H7... O19, (c), H7... O20 and (f), H12... O18. The corresponding bond lengths and bond angles are 2.49 Å, 2.5091 Å, and 2.0594 Å, and 174.684^0, 174.7009^0, and 120.61532^0, respectively. A strong H-bond corresponding to a stable geometrical model of complex can be shown in Figure 6(f). However, the interaction energy of enthalpy for complex (f) is -21.77 kcal/mol, and its interaction shows chemisorption of CO_2. The charge transfer from anions to CO_2 and the change of angle formed between C and O are included in this computational investigation in the formation of all of the anions-CO_2 complexes and summarized in Table 3 as follows.

Table 3. *Bending angle (<O-C-O^0) and Muliken charge distribution of both anion-CO_2 complexes are presented here in the gas phase at M062X/6-31+G (d, p) level.*

	Complexes	Charge distribution	Bending angle
(a')	$[C_6H_4NS_2O_4]$-CO_2 I (a)	-1.465	174.777
	$[C_6H_4NS_2O_4]$-CO_2 II (b)	-1.481	174.684
	$[C_6H_4NS_2O_4]$-CO_2 III(c)	-1.481	174.70091
	$[C_6H_4NS_2O_4]$-CO_2 IV (d)	-1.639	175.818
(b')	$[C_8H_4NO_2]$-CO_2 I (e)	-0.68	138.37007
	$[C_8H_4NO_2]$-CO_2 II (f)	-0.579	120.61532
	$[C_8H_4NO_2]$-CO_2 III (g)	-0.689	177.29593

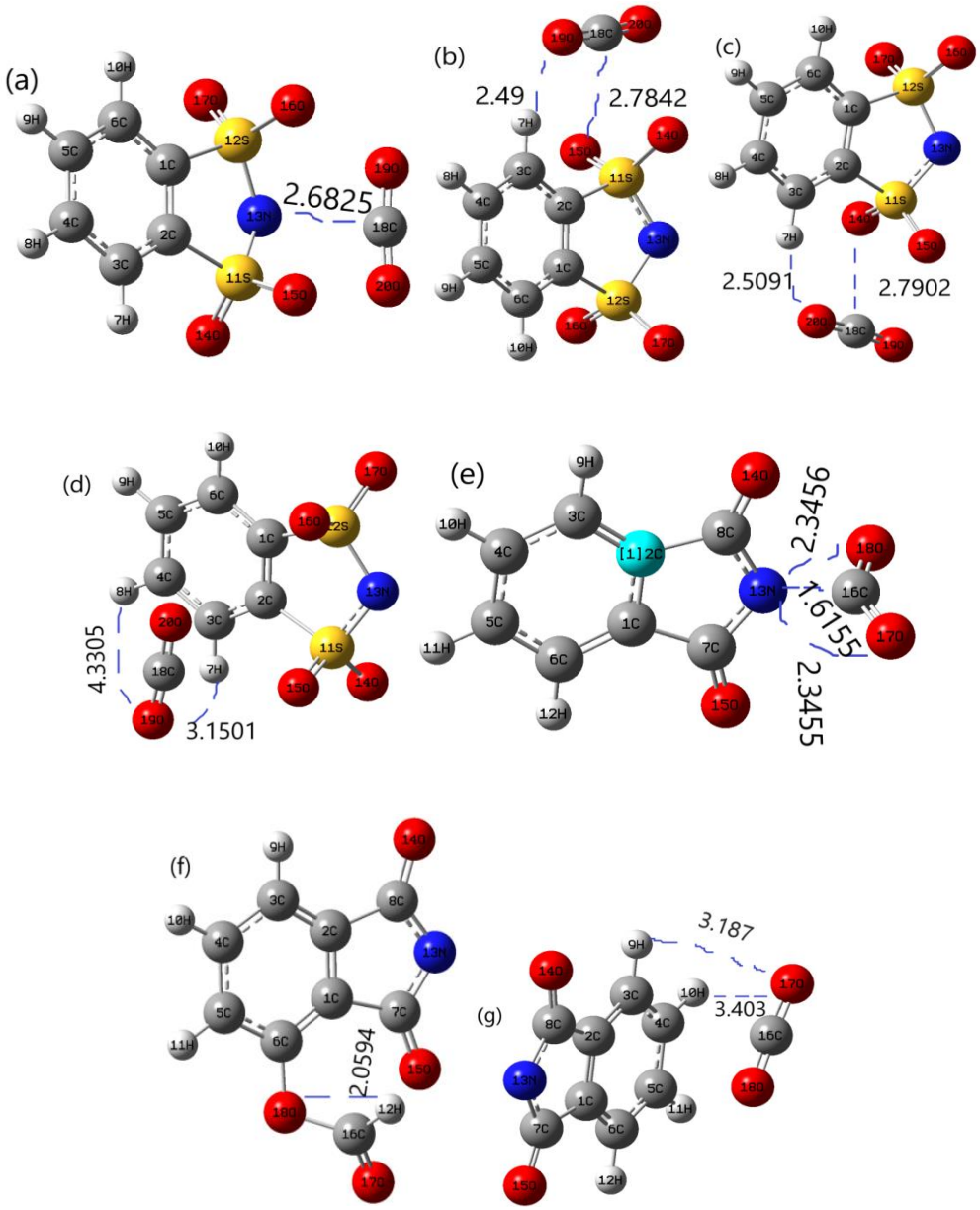

Figure 6. *The optimized structures of $[C_8H_4NO_2]$-CO_2 and $[C_6H_4NS_2O_4]$-CO_2 complexes in gas phase calculated at M062X/6-31+G (d, p) level.*

The ESP map of $[C_6H_4NS_2O_4]$ -CO_2 and $[C_8H_4NO_2]$ -CO_2 complexes are shown in Figure 7. It can be easily shown that the ESP surface sites close to the molecular interactions were affected by the stereo structure and the charge density distribution. The highly negative regions (red area) in the ESP surface of both anions and CO_2 were found away from one another and showed high activity around the high abundance of electron-rich parts of atoms present in the anions-CO_2 complex. In contrast, the highly positive regions (yellow area) in each part of the anions- CO_2 complexes were localized on the hydrocarbon bonds, which could be considered a possible site for nucleophilic attack of the C-atom in the CO_2 molecule. The C- atom in CO_2 attacking the N13, H12, and all parts of the O atoms of each anion were determined by ESP analysis, which coincides with the following quantum chemical analysis of this computational study.

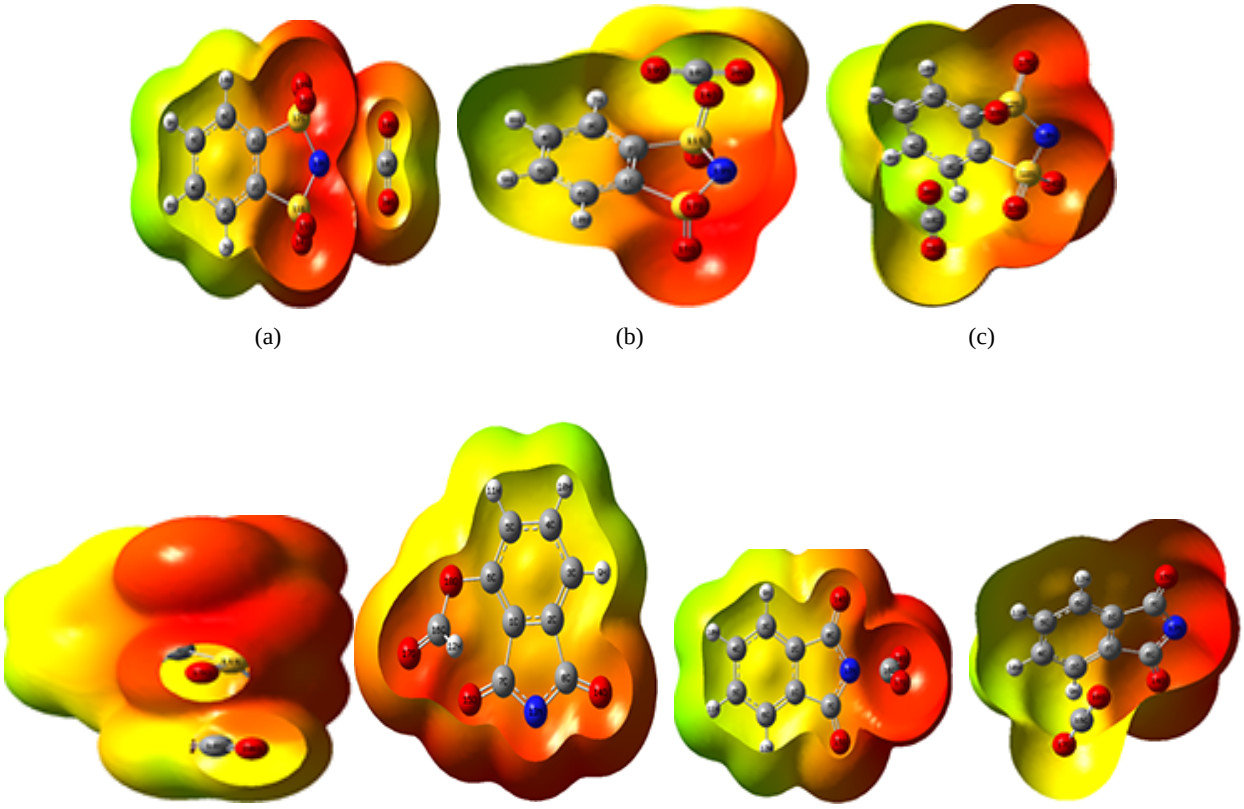

Figure 7. *The ESP map of $[C_8H_4NO_2]$-CO_2 and $[C_6H_4NS_2O_4]$-CO_2 complexes in the gas phase calculated at M062X/6-31+G (d, p) level.*

3.4. Interaction of IL Pair with CO_2

The capacity of absorption of CO_2 in the ILs was noteworthy for further study. This may possibly be related to the computational interactions between ILs and CO_2 molecules. In this work, based on related previous power-driven reports [31] and the DFT-based optimized geometries, the two interaction mechanisms (Scheme 3 and 4) were proposed to show the formation of ILs-CO_2 complexes. Mechanisms of IL with CO_2 interactions are shown in Schemes 3 and 4 below.

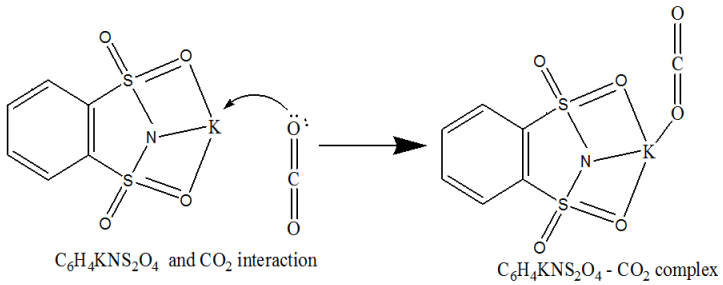

Scheme 3. *The interaction mechanism between $C_6H_4KNS_2O_4$ and CO_2.*

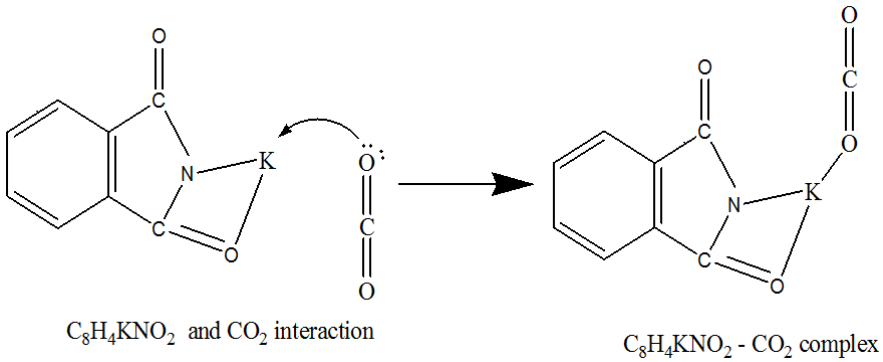

Scheme 4. *The interaction mechanism between $C_8H_4KNO_2$ with CO_2.*

The interaction of two IL, $C_8H_4KNO_2$ and $C_6H_4KNS_2O_4$ with CO_2 were investigated using quantum chemical calculations. The geometries of ILs were optimized at the M062X/6-31+G (d,p) level, and vibrational frequency analysis confirmed stable structures with no imaginary frequencies. The IL-CO_2 complexes were also optimized to study the interactions, and thermochemical data, including binding energies and other relevant parameters, were compiled in Table 4. This study provides insights into the roles of CO_2 in the absorption process by these ILs.

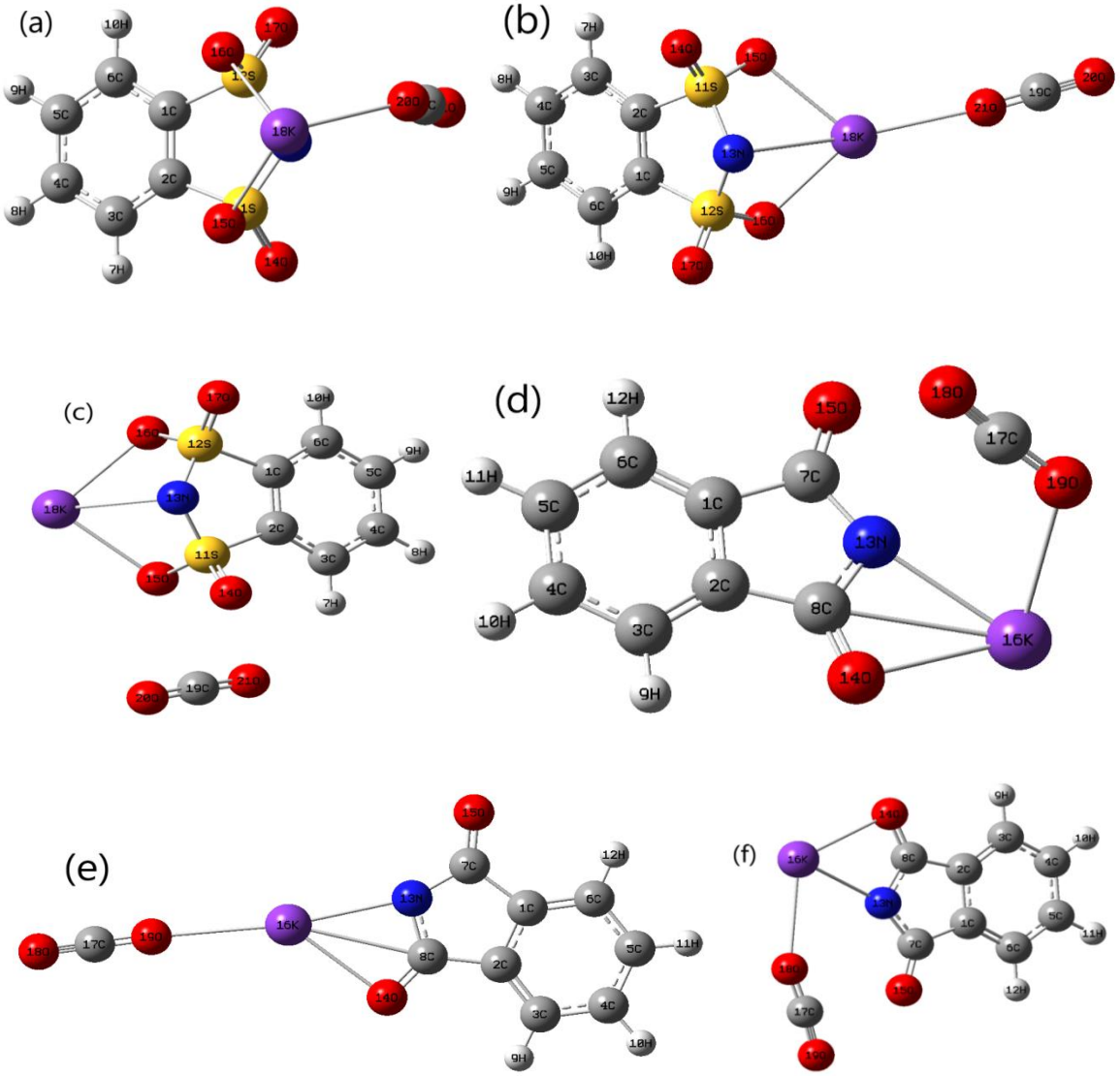

Figure 8. *Optimized minimum energy structural IL-CO_2 complexes are calculated at M062X/6-31+G(d,p) level in gas.*

The interaction between ILs and CO_2 were studied by first optimizing the geometry of each component individually using the M062X/6-31+G(d,p) level of theory. CO_2 was then placed in high electron density regions around the optimized IL structure, and the IL- CO_2 complexes were calculated using Gaussian 09 software. Six stable geometries of IL- CO_2 complexes were obtained, confirmed by the absence of imaginary frequencies. Electrostatic potential (ESP) maps of these complexes were generated, revealing additional binding sites where IL- CO_2 interactions may occur.

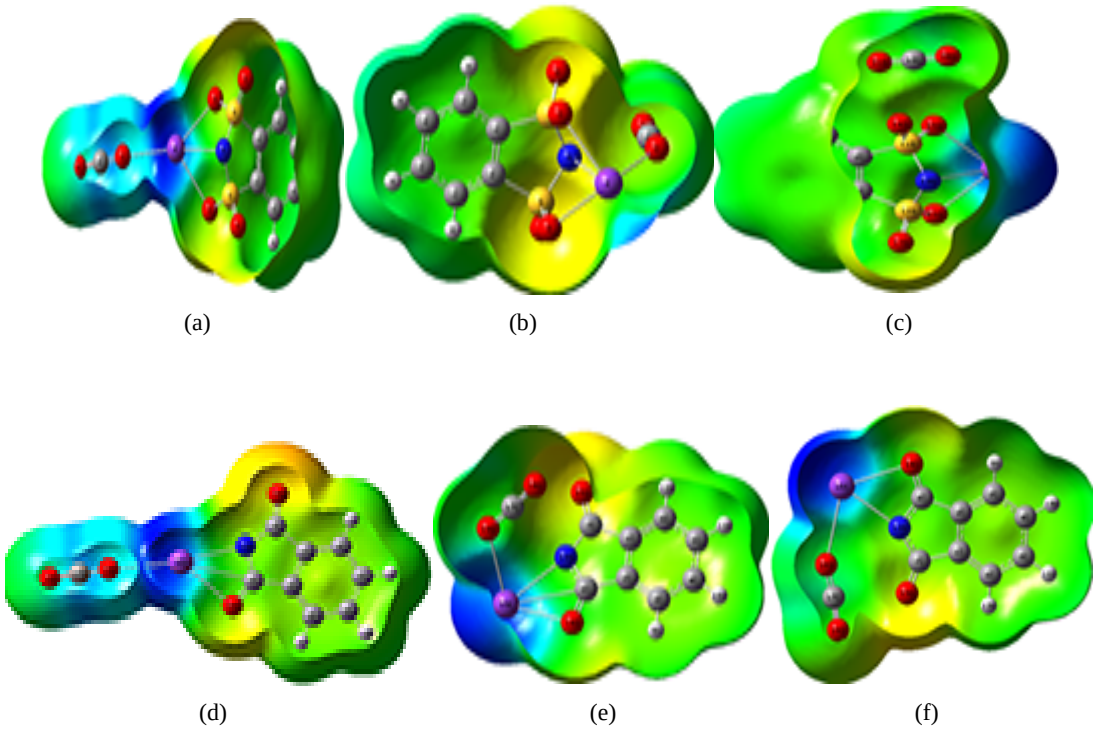

Figure 9. *The ESP map of $C_6H_4KNS_2O_4$-CO_2 and $C_8H_4KNO_2$-CO_2 complexes calculated at M062X/6-31+G(d,p) level in gas phase.*

Table 4. *Geometrical parameters and thermochemical data for the minimum energy structural ILs-CO_2 conformers at M062X/6-31+G(d,p) level in gas phase.*

Thermodynamic values	**$C_6H_4KNS_2O_4$ -CO_2 Conformer**			**$C_8H_4KNO_2$ -CO_2 Conformer**		
	(a)	**(b)**	**(c)**	**(d)**	**(e)**	**(f)**
C−O, Å	1.1544	1.1561	1.165	1.155	1.156	1.17
< O-C-O, ^{0}	176.53	179.92	177.13	175.45	179.93	174.5
Relative energy, kcal mol^{-1}	1.0000	0.000	1.000	1.000	1.000	0.000
ΔB.E, kcal mol^{-1}	-25.989	-21.585	-23.58	-26.15	-21.42	-25.85
ΔH, kcal mol^{-1}	-26.5813	-22.177	-24.172	-26.74	-22.01	-26.44
ΔS, cal mol^{-1}k^{-1}	-27.406	-21.497	-28.88	-28.00	-20.22	-25.18
Dpm, Debye	6.44	8.07	6.93	7.15	9.05	7.04

The interaction between ILs and CO_2, specifically involving potassium ion, results in the formation of carbamate bonds. Computational calculations using Gaussian software show that the formation of these bonds is energetically favorable, with exothermic enthalpy changes (ΔH). The ion pair $C_6H_4KNS_2O_4$ exhibits lower ΔH, indicating it is more efficient for CO_2 absorption and regeneration compared to $C_8H_4KNO_2$, making it a potentially environmentally friendly

option for CO_2 chemisorption. The interaction leads to a bending of CO_2's typical linear structure, with the O-C-O bond angle adjusting based on the specific IL-CO_2 complex formed. The study also evaluates the ion pairing energy ($\Delta B.EIL\text{-}CO_2$), further demonstrating the stability of the ion pair.

In the chemisorption between the O atom in CO_2 and the K atom for both ILs, compared to 180^0 of the pure CO_2 molecule, the angle of O=C=O was the bending degree of O=C=O from 180^0 to 176.53^0 (a), 179.92^0 (b) and 177.13^0 (c), and the bond length between C and O was extended from 1.1544 Å (a) to 1.1561 Å (b) and 1.1565 Å (c) all in the optimized structures of $C_6H_4KNS_2O_4$ - CO_2 complexes, respectively. In the same way, the angle of O=C=O was bent to 175.45^0 (d), 179.93^0 (e), and 174.5^0 (f) with extended bond lengths of 1.155 Å (d), 1.156 Å (e), and 1.17 Å (f) in $C_8H_4KNO_2$ - CO_2 complexes, respectively. All IL-CO_2 complexes were calculated at the M062X/6-31+G(d,p) level of theory in the absence of imaginary frequency. Consequently, complexes (b), (c), and (e) are capable of absorbing CO_2 molecules at the three major possible sites due to the observation of lower ΔH, which is shown in Figure 8. The interaction of CO_2 with $C_6H_4KNS_2O_4$ is more favorable at a lower ΔH value relative to $C_8H_4KNO_2$. This computational investigation result of the angle of bending CO_2 in the interaction with both IL optimized geometry of (b), (c), and (e) are better than more recent work such as the phenolic IL with CO_2 experimental observations to 177^0 reported by Vafaeezadeh and his co-workers [32]. The optimized structures in Figure 8 also suggest that the [K] cation and [$C_6H_4NS_2O_4$] anion in the ion pair have active sites for CO_2 absorption. It was found that the [K] cation and [$C_6H_4NS_2O_4$] anion were the main active sites for the loading of CO_2.

3.5. NBO Analysis

Table 5. *The main second order perturbation stabilization energy, E(2) (Kcal/mol) of accepter and donor in $C_8H_4KNO_2$, $CO_2/C_8H_4KNO_2$, $C_6H_4KNS_2O_4$ and $CO_2/C_6H_4KNS_2O_4$ complexes calculated at M062X/ 6-31+G(d, p) level in the gas phase as follow.*

Species	Donor(i)	Accepter(j)	E2(kcal/mol)	Ej-Ei/a.u
$C_8H_4KNO_2$	LP1(N13)	BD*1(C2-C8)	11.45	1.24
	LP2(O14)	BD*1(C2-C8)	25.88	1.12
	LP2(O14)	BD*1(C8-N13)	24.20	1.23
	LP2(O14)	BD*1(C8-N13)	24.20	1.23
	LP2(O 14)	BD*1(C8-N13)	24.20	1.23
	LP2(O15)	BD*1(C7-N13)	32.00	1.16
$CO_2/C_8H_4KNO_2$	LP2(O14)	BD*1(C2-C8)	26.15	1.12
	LP2(O14)	BD*1(C8-N13)	24.51	1.23
	LP2(O15)	BD*1(C1-C7)	28.81	1.09
	LP2(O15)	BD*1(C7-N13)	31.88	1.16
	LP3(O15)	BD*2(C7-N13)	266.99	0.42
$C_6H_4KNS_2O_4$	LP2(N13)	BD*1(S11-O15)	18.54	0.62
	LP2(O14)	BD*1(S11-O15)	30.66	0.66
	LP3(O14)	BD*1(C2-S11)	22.13	0.54
	LP2(O15)	BD*1(S11-N13)	22.69	0.63
	LP3(O15)	BD*1(C2-S11)	20.46	0.56
	LP2(O16)	BD*1(S12-N13)	22.70	0.63
	LP3(O16)	BD*1(C1-S12)	20.47	0.56
	LP2(O17)	BD*1(S12-O16)	30.66	0.66
	LP3(O17)	BD*1(C1-S12)	22.12	0.54
	LP3(O17)	BD*1(S12-N13)	21.52	0.60

Species	Donor(i)	Accepter(j)	E2(kcal/mol)	Ej-Ei/a.u
$CO_2/C_6H_4KNS_2O_4$	LP2(O14)	BD*1(S11-O15)	33.06	0.96
	LP3(O14)	BD*1(C2-S11)	24.37	0.80
	LP3(O14)	BD*1(S11-N13)	23.38	0.87
	LP2(O15)	BD*1(S11-N13)	25.39	0.90
	LP3(O15)	BD*1(C2-S11)	22.66	0.82
	LP2(O16)	BD*1(S12-N13)	25.72	0.90
	LP3(O16)	BD*1(C1-S12)	22.22	0.82
	LP2(O17)	BD*1(S12-O16)	32.40	0.96
	LP3(O17)	BD*1(C1-S12)	26.73	0.80
	LP3(O17)	BD*1(S12-N13)	20.09	0.87

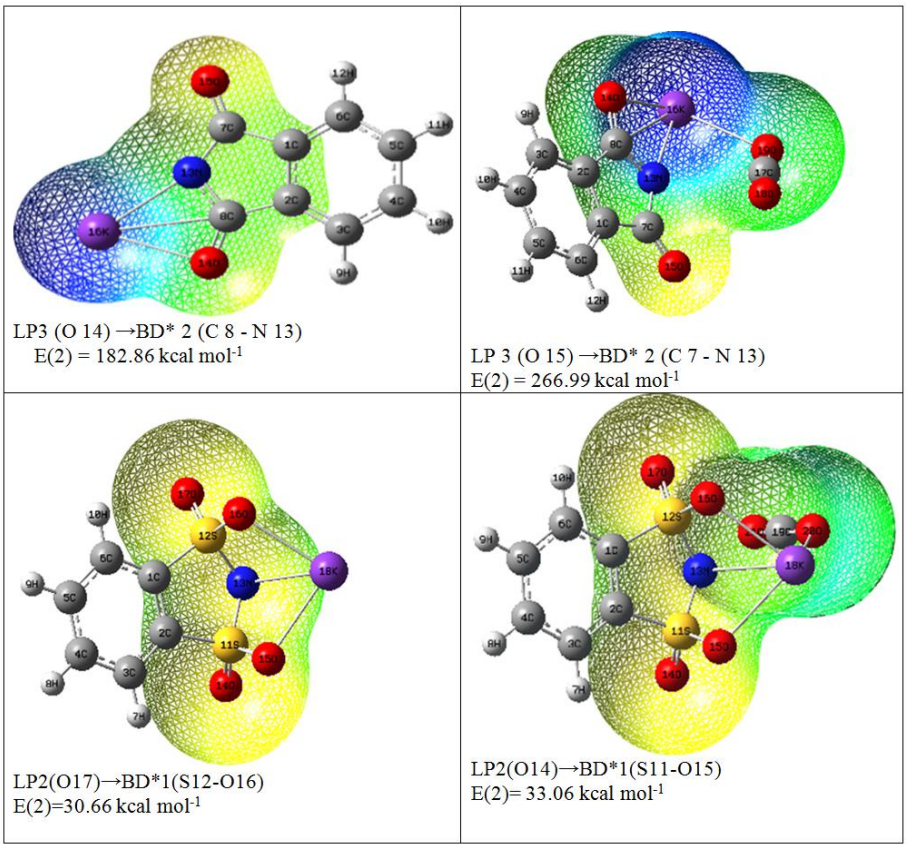

Figure 10. *The schematic graphs of the charge transfer occurring from the lone-pairs to the anti-bonding orbital based on the NBO analysis at M062X/6-31+G(d,p) level.*

The NBO analysis was sustained by showing the minimum energy structures of $C_8H_4KNO_2$, $C_6H_4KNS_2O_4$ and the best selected geometry of IL- CO_2 conformers in gas phase from Figure 8(a) and (d) above by using M062X/6- 31+G(d, p) level. In order to define the charge transfer taking place from the ion pairs to the anti-bonding orbital, the main donor-accepter orbitals are shown in Figure 10. The main second-order perturbation stabilization energy, E(2) (kcal/mol), of accepter and donor in two ILs and ILs - CO_2 and the data of NBO in relation to these discussions are shown in Table 5. The advanced the numerical value E(2), the better the interface strength between the donor and acceptor atoms in a molecule. As shown in Table 5, for $C_8H_4KNO_2$, E(2) of LP3 (O14) → BD* 2 (C8- N13) is 182.86 kcal/mol, and it indicates the existence of a very strong interaction between the orbitals of LP 3(O14) and BD*2 (C7-O15). At the same time, the

E(2)s of LP 2 (O15) → BD*1 (C7-N13) and LP 2 (O15) → BD*1 (C1-C7) are 32.00 and 28.78 kcal/mol, respectively. It suggests that the increasing order interactions between the donors and accepters are LP 2 (O15) → BD* 1 (C1-C7) < LP 2 (O15) → BD*1 (C7-N13) < LP3 (O14) → BD* 2 (C8-N13). In $CO_2/C_8H_4KNO_2$ complexes, the E(2)s of LP 3 (O15) → BD* 2 (C7 - N13) are 266.99 kcal/mol, which shows an extremely strong interaction between the orbitals of LP 2 (O15) → BD*1 (C7 - N13). For the $C_6H_4KNS_2O_4$, E(2) of LP 2 (O14) → BD* 1 (S11 - O15) and LP 2 (O17) → BD* 1 (S12 - O16) are 30.66 kcal/mol, and it shows better interaction between the orbital's of LP2 (O14) and BD* 1 (S11 - O15), LP2 (O17) and BD* 1 (S12-N13) than the other donor-accepter orbital's of atoms in this ionic pair. Generally, the values of E(2)s are large and strong orbital interactions in $CO_2/C_8H_4KNO_2$ complexes than $C_8H_4KNO_2$, $C_6H_4KNS_2O_4$ and $CO_2/C_6H_4KNS_2O_4$. All types of this computational analysis are carried out by investigating all possible interactions, donor NBO (i) and acceptor NBO (j), stabilization energy E(2) connected with delocalization, or two electron stabilizations [30].

3.6. Solvent Effect on Interactions of IL...CO_2 Complexes

The solvent effects were considered to minimize potential biases in the quantum chemical computations. Using the PCM model [22], all species and complexes were re-optimized at the M062X/6-31+G(d,p) level in the presence of three solvents—water, DMSO, and chloroform. Unlike the gas-phase calculations, solvent inclusion did not significantly alter the geometry of the anion-CO_2 complexes. However, the thermochemical properties of the species and complexes were notably affected by the solvents, as revealed by the quantum chemical calculations [32].

Table 6. *Solvents effect on anion- CO_2 complexes thermochemical data in unit of Kcal/mol for ΔH, ΔB.E, and Cal/ molk for ΔS at M062X/6-31+G(d,p) level.*

(a) $[C_8H_4NO_2]$ - CO_2 complexes

	Chloroform			DMSO			Water		
	ΔH	ΔB.E	ΔS	ΔH	ΔB.E	ΔS	ΔH	ΔB.E	ΔS
I	-7.26	-6.67	-35.1	-8.08	-7.19	-35.55	-8.13	-7.54	-35.54
II	13.74	14.3	-36.21	14.47	15.06	-36.43	14.48	15.07	-36.35
III	-1.73	-1.139	-24.04	-1.51	-0.92	-23.09	-1.5	-0.913	-22.63

(b) $[C_6H_4NS_2O_4]$ - CO_2 complexes

	Chloroform			DMSO			Water		
	ΔH	ΔB.E	ΔS	ΔH	ΔB.E	ΔS	ΔH	ΔB.E	ΔS
I	-3.01	-2.42	-29.53	-2.7	-2.11	-26.51	-2.69	-2.10	-26.25
II	-3.8	-3.21	-29.33	-3.04	-2.45	-27.69	-3.009	-2.41	-27.74
III	-3.81	-3.22	-27.099	-3.003	-2.41	-27.99	-2.97	-2.377	-28.13
IV	-3.22	-2.634	-29.84	-2.94	-2.35	-29.12	-2.94	-2.35	-29.17

The effect of three solvents on the geometry, binding energies, and interactions of ion pairs in the gas phases of IL-CO_2 complexes has been re-optimized. Table 7 provides a summary of the thermochemical information about $C_8H_4KNO_2$ and $C_6H_4KNS_2O_4$ ILs in terms of ΔH, ΔB.E (kcal/ mol), and ΔS (cal /molk).

Table 7. *The thermodynamic data for $C_8H_4KNO_2$ and $C_6H_4KNS_2O_4$ ILs in the presence of selected solvents at M062X/6-31+G(d,p) level.*

Chloroform				**DMSO**			**Water**		
ILs	**ΔH**	**ΔB.E**	**ΔS**	**ΔH**	**ΔB.E**	**ΔS**	**ΔH**	**ΔB.E**	**ΔS**
$C_6H_4KNS_2O_4$	-28.11	-20.7	-26.5	-8.806	-8.21	-25.46	-7.91	-7.32	-25.48
$C_8H_4KNO_2$	-30.04	-29.45	-24.0	-9.69	-9.10	-23.11	-8.78	-8.19	-23.05

Quantum chemical computations show that solvent effects can significantly alter molecular interactions compared to gas-phase data. Chloroform exhibits stronger bonding and greater stability for ion-pair interactions (−26.59 cal/mol·K) compared to water (−25.48 cal/mol·K) and DMSO (−25.46 cal/mol·K). This suggests chloroform better stabilizes certain cation-anion pairs. Water, however, remains a preferred solvent for ILs due to its ability to lower energy requirements for CO_2 absorption and IL regeneration, likely due to its polarity and hydrogen bonding capabilities.

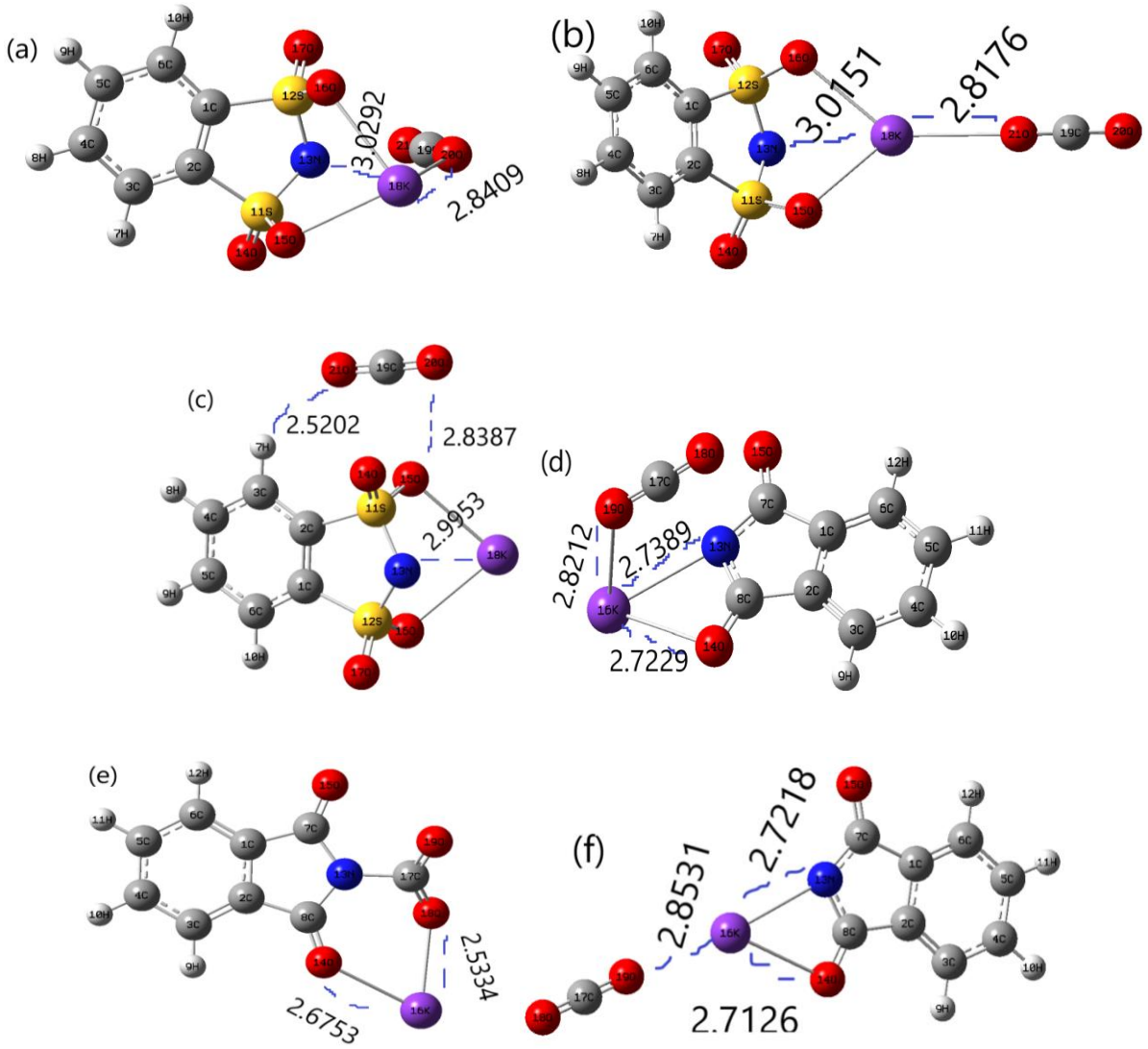

Figure 11. *Solvents effect on the geometries of (a-c) and (d-f) complexes of $C_6H_4KNS_2O_4$ and $C_8H_4KNO_2$ with CO_2 were calculated by polarized continuum model (PCM) at M062X/6-31+G(d,p) level.*

The study investigates the interaction between CO_2 and two ILs, $C_6H_4KNS_2O_4$ and $C_8H_4KNO_2$, focusing on their interaction energies in both gas and solvent phases. The K^+ cation in both ILs shows a strong interaction with CO_2, especially in $C_6H_4KNS_2O_4$. Interaction energies calculated using the Polarizable Continuum Model (PCM) are between -3.69 and -0.049 kcal/mol in the solvent phase, which is lower than the gas-phase values (-22.177 and -22.01 kcal/mol). The results are reasonable agree with −16.8 kJ/mol or -4.019 kcal mol^{-1} of $[NH_2emim][BF_4]$−CO_2 system reported by Wu et al., [33]. $C_6H_4KNS_2O_4$ interacts slightly more strongly with CO_2 than $C_8H_4KNO_2$ in solution. These results are consistent with prior studies, suggesting competitive absorption behavior of CO_2 with both ILs.

Table 8. *Solvent effects on IL- CO_2 complexes thermochemical data in unit Kcal/ mol for ΔH, ΔB.E and Cal/molK for ΔS at M062X/6-31+G(d,p) level.*

	Chloroform			DMSO			Water		
	ΔH	**ΔB.E**	**ΔS**	**ΔH**	**ΔB.E**	**ΔS**	**ΔH**	**ΔB.E**	**ΔS**
(a)	-3.69	-3.108	-24.98	-3.05	-2.465	-26.63	-3.02	-2.435	-26.66
(b)	-0.82	-0.232	-21.40	-0.049	0.542	-18.62	0.025	0.618	-20.56
(c)	-3.51	-2.922	-26.40	-2.828	-2.235	-25.97	-2.81	-2.221	-26.89
(d)	-4.06	-3.475	-27.39	-3.23	-2.644	-27.19	-3.19	-2.605	-28.79
(e)	-0.811	-0.219	-19.12	0.075	0.668	-19.65	0.11	0.703	-19.62
(f)	-2.809	-2.218	-22.83	-1.65	-1.063	-22.84	-1.6	-1.014	-23.17

The study uses DFT to compute the binding energies of ILs-CO_2 complexes, with results ranging from -3.475 to -0.219 kcal/mol, in good agreement with experimental data from Tilvet et al [34] (binding energy of -2.7 kcal/mol). The binding energy is influenced by the solvent, with chloroform found to be the most effective for reducing binding energy and facilitating CO_2 absorption. The interaction between the electrophilic potassium ion (K) and the nucleophilic oxygen (O) of CO_2 is analyzed, showing that shorter bond lengths indicate stronger interactions. The strongest interactions occur in the dIL and bIL conformers, while strong hydrogen bonding is observed in the cIL conformer. Overall, the study demonstrates that DFT calculations effectively predict IL-CO_2 binding and interaction strengths.

4. Conclusion

In this work, for $C_6H_4KNS_2O_4$ and $C_8H_4KNO_2$ IL-based CO_2 absorption has been examined with the objective of clarifying phases to analyze and report the absorption process by using the DFT method of mixed M062X and 6-31+G(d,p) levels, which leads to the design of more effective IL absorbents. The calculated binding energies are in the range of 3.108 kcal/mol to-0.232 kcal/mol for $C_6H_4KNS_2O_4$ and-3.475 kcal/mol to-0.219 kcal/mol for $C_8H_4KNO_2$ for the preferred complexes in the presence of solvents. These results imply the existence of interaction between the CO_2 and the IL pair. The IL can absorb CO_2 effectively, and the energy consumption for its regeneration is low. The interaction between CO_2 and IL pairs of both ILs causes a change in their some geometrical parameters. The NBO analysis predicts the transferred charges between the ion pair and CO_2 in terms of determining the second-order perturbation stabilization energies. In this computational investigation, it would be beneficial to consider ILs in which carbamate bond formation occurs but are energetically costly and not environmentally friendly for an absorption process. In this case, all of the systems were studied under the solvent effect (i.e., chloroform, DMSO, and water) to reduce unrealistic effects in this computational investigation. From the interactions of none of the ILs (anion-CO_2 complexes), $[C_8H_4NO_2]$-CO_2(I), $[C_6H_4NS_2O_4]$-CO_2 (II), and $[C_6H_4NS_2O_4]$-CO_2 (III) complexes were a realistic replacement for $C_6H_4KNS_2O_4$ and $C_8H_4KNO_2$ solvents in the selected solvent phase system in this study due to higher chemisorption of CO_2. Overall, our calculations indicate the existence of these stable complexes between the IL pairs and CO_2 molecules. $C_6H_4KNS_2O_4$ IL is more suitable for absorption of CO_2.

Abbreviations

DFT	Density Functional Theory
DMSO	Dimethyl Sulfoxide
E2	Second-Order Perturbation Stabilization Energies
ESP	Electrostatic Potential
HOMO	Highest Occupied Molecular Orbital
ILs	Ionic Liquids
LUMO	Lowest Unoccupied Molecular Orbital
MEA	Monoethanol Amine
MESP	Molecular Electrostatic Potential
NBO	Natural Bond Orbital
PCM	Polarizable Continuum Model
SCRF	Self-Consistent Reaction Field

Acknowledgments

First and foremost, I want to express my enormous thanks to the almighty God for the gift of life, wisdom, and understanding he has given me, a reason for my existence, and for passing safely through the many difficulties of this journey. The success of this research would have been difficult without the help and continuous guidance of certain people. I hereby take the chance to thank a few people for their help, guidance,

and encouragement in the successful completion of my research. First, I would like to thank my advisor, Dr. Endale (Ph.D.), for giving me the opportunity to do this work to pursue my M.Sc. degree at the department and for continuous trustworthy advice, support, interesting discussions, and giving me freedom in choosing how to approach different issues. Secondly, I would like to express my thanks to my co-advisor, Abdudin Geremu (M.Sc.), for his interest, encouragement, appreciation, and valuable advice from the selection of the research title to all phases of my work. I would also like to thank people in the Department of Chemistry, in particular in the physical chemistry stream, for providing a good working chemistry computer lab. A special thank you goes to Abdudin Geremu (M.Sc.) for first introducing me to computational chemistry, experimental setups, experimental work, and data acquisition systems up to the final of this study. Finally, I would like to thank my family for always being there and financially supporting me during the year of my study.

Author Contributions

Berihun Tibebu: Conceptualization, Data curation, Investigation, Methodology, Validation, Writing – original draft

Abdudin Geremu: Conceptualization, Data curation, Investigation, Project administration, Software, Validation, Writing – review & editing

Endale Tsegaye: Conceptualization, Data curation, Project administration, Supervision, Validation, Writing – review & editing

Conflicts of Interest

The authors declare no conflicts of interest.

References

[1] Y. Zhang, X. Lu and X. Ji, *Carbon dioxide capture*, Deep Eutectic Solvents Synth. Prop. Appl. (2019), pp. 297-319. http://dx.doi.org/10.1002/9783527818488.ch15

[2] S. Harrison, J. Franklin, R. R. Hernandez, M. Ikegami, H. D. Safford and J. H. Thorne, *Climate change and California's terrestrial biodiversity*, Proc. Natl. Acad. Sci. 121 (2024), pp. e2310074121. https://doi.org/10.1073/pnas.2310074121

[3] T. M. Gür, *Carbon dioxide emissions, capture, storage and utilization: Review of materials, processes and technologies*, Prog. Energy Combust. Sci. 89 (2022), pp. 100965. https://doi.org/10.1016/j.pecs.2021.100965

[4] M. C. Stern, F. Simeon, H. Herzog and T. A. Hatton, *Post-combustion carbon dioxide capture using electrochemically mediated amine regeneration*, Energy Environ. Sci. 6 (2013), pp. 2505-2517. https://doi.org/10.1039/C3EE41165F

[5] F. Wang, S. Deng, H. Zhang, J. Wang, J. Zhao, H. Miao et al., *A comprehensive review on high-temperature fuel cells with carbon capture*, Appl. Energy 275 (2020), pp. 115342. https://doi.org/10.1016/j.apenergy.2020.115342

[6] M. Freemantle, *Ionic liquids may boost clean technology development*, Chem Eng News 76 (1998), pp. 32-37. https://doi.org/10.1021/CEN-V076N013.P032

[7] X. Fan, S. Liu, Z. Jia, J. J. Koh, J. C. C. Yeo, C.-G. Wang et al., *Ionogels: recent advances in design, material properties and emerging biomedical applications*, Chem. Soc. Rev. 52 (2023), pp. 2497-2527. https://doi.org/10.1039/D2CS00652A

[8] J. Cao, D. Zhang, X. Zhang, Z. Zeng, J. Qin and Y. Huang, *Strategies of regulating Zn 2+ solvation structures for dendrite-free and side reaction-suppressed zinc-ion batteries*, Energy Environ. Sci. 15 (2022), pp. 499-528. https://doi.org/10.1039/D1EE03377H

[9] L. A. Blanchard, D. Hancu, E. J. Beckman and J. F. Brennecke, *Green processing using ionic liquids and CO2*, Nature 399 (1999), pp. 28-29. http://dx.doi.org/10.1038/19887

[10] B. Xue, Y. Yu, J. Chen, X. Luo and M. Wang, *A comparative study of MEA and DEA for post-combustion CO 2 capture with different process configurations*, Int. J. Coal Sci. Technol. 4 (2017), pp. 15-24. http://dx.doi.org/10.1007/s40789-016-0149-7

[11] F. Vega, S. Camino, J. Camino, J. Garrido and B. Navarrete, *Partial oxy-combustion technology for energy efficient CO2 capture process*, Appl. Energy 253 (2019), pp. 113519. https://doi.org/10.1016/j.apenergy.2019.113519

[12] F. U. Shah, R. An and N. Muhammad, *Properties and applications of ionic liquids in energy and environmental science*, Front. Chem. 8 (2020), pp. 627213. https://doi.org/10.3389/fchem.2020.627213

[13] D. Bâlint and L. Jäntschi, *Comparison of molecular geometry optimization methods based on molecular descriptors*, Mathematics 9 (2021), pp. 2855. https://doi.org/10.3390/math9222855

[14] J. J. Stewart, *Application of the PM6 method to modeling the solid state*, J. Mol. Model. 14 (2008), pp. 499-535. http://dx.doi.org/10.1007/s00894-008-0299-7

[15] N. S. Babu, *Applications of Current Density Functional Theory (DFT) Methods in Polymer Solar Cells*, in *Density Functional Theory-Recent Advances, New Perspectives and Applications*, IntechOpen, 2021. https://doi.org/10.5772/intechopen.100136

[16] V. A. Rassolov, M. A. Ratner, J. A. Pople, P. C. Redfern and L. A. Curtiss, *6-31G* basis set for third-row atoms*, J. Comput. Chem. 22 (2001), pp. 976-984. https://onlinelibrary.wiley.com/doi/10.1002/jcc.1058

[17] Y. Sert, L. Singer, M. Findlater, H. Doğan and Ç. Çırak, *Vibrational frequency analysis, FT-IR, DFT and M06-2X studies on tert-Butyl N-(thiophen-2yl) carbamate*, Spectrochim. Acta. A. Mol. Biomol. Spectrosc. 128 (2014), pp. 46-53. https://doi.org/10.1016/j.saa.2014.02.114

[18] M. Mercy, N. H. de Leeuw and R. G. Bell, *Mechanisms of CO 2 capture in ionic liquids: a computational perspective*, Faraday Discuss. 192 (2016), pp. 479-492. https://doi.org/10.1039/C6FD00081A,

[19] B. Lai and C. Oostenbrink, *Binding free energy, energy and entropy calculations using simple model systems*, Theor. Chem. Acc. 131 (2012), pp. 1-13. http://dx.doi.org/10.1007/s00214-012-1272-1

[20] R. Gangadharan and S. Sampath Krishnan, *Natural Bond Orbital (NBO) population analysis of 1-azanapthalene-8-ol*, Acta Phys. Pol. A 125 (2014), pp. 18-22. http://dx.doi.org/10.12693/APhysPolA.125.18

[21] B. Cao, J. Du, S. Liu, X. Zhu, X. Sun, H. Sun et al., *Carbon dioxide capture by amino-functionalized ionic liquids: DFT based theoretical analysis substantiated by FT-IR investigation*, RSC Adv. 6 (2016), pp. 10462-10470. https://doi.org/10.1039/C5RA23959A

[22] K. Dhar and S. Fahim, *Investigation of the Absorption of CO2 in Ionic Liquid*, Bangladesh J. Sci. Res. 29 (2016), pp. 41-46. https://doi.org/10.3329/bjsr.v29i1.29756

[23] D. Josa, J. Rodríguez-Otero, E. M. Cabaleiro-Lago and M. Rellán-Piñeiro, *Analysis of the performance of DFT-D, M05-2X and M06-2X functionals for studying π⋯ π interactions*, Chem. Phys. Lett. 557 (2013), pp. 170-175. https://doi.org/10.1016/j.cplett.2012.12.017

[24] Y. Wang, P. Verma, X. Jin, D. G. Truhlar and X. He, *Revised M06 density functional for main-group and transition-metal chemistry*, Proc. Natl. Acad. Sci. 115 (2018), pp. 10257-10262. https://doi.org/10.1073/pnas.1810421115

[25] V. Lachet, T. de Bruin, P. Ungerer, C. Coquelet, A. Valtz, V. Hasanov et al., *Thermodynamic behavior of the CO2+ SO2 mixture: Experimental and Monte Carlo simulation studies*, Energy Procedia 1 (2009), pp. 1641-1647. https://doi.org/10.1016/j.egypro.2009.01.215

[26] M. B. Shiflett and Ajj. Yokozeki, *Phase behavior of carbon dioxide in ionic liquids: [emim][acetate], [emim][trifluoroacetate], and [emim][acetate]+[emim][trifluoroacetate] mixtures*, J. Chem. Eng. Data 54 (2009), pp. 108-114. https://doi.org/10.1021/je800701j

[27] V. E. Romanovsky, D. Drozdov, N. G. Oberman, G. Malkova, A. L. Kholodov, S. Marchenko et al., *Thermal state of permafrost in Russia*, Permafr. Periglac. Process. 21 (2010), pp. 136-155. https://doi.org/10.1002/ppp.683

[28] B. Shimekit and H. Mukhtar, *Natural gas purification technologies-major advances for CO2 separation and future directions*, Adv. Nat. Gas Technol. 2012 (2012), pp. 235-270. https://www.intechopen.com/chapters/35293

[29] J. A. Keith, V. Vassilev-Galindo, B. Cheng, S. Chmiela, M. Gastegger, K.-R. Muller et al., *Combining machine learning and computational chemistry for predictive insights into chemical systems*, Chem. Rev. 121 (2021), pp. 9816-9872. https://doi.org/10.1021/acs.chemrev.1c00107

[30] H. Sun, B. Cao, Q. Tian, S. Liu, D. Du, Z. Xue et al., *A DFT study on the absorption mechanism of vinyl chloride by ionic liquids*, J. Mol. Liq. 215 (2016), pp. 496-502. https://doi.org/10.1016/j.molliq.2016.01.026

[31] Mukhtar, S. Saqib, N. B. Mellon, M. Babar, S. Rafiq, S. Ullah et al., *CO2 capturing, thermo-kinetic principles, synthesis and amine functionalization of covalent organic polymers for CO2 separation from natural gas: A review*, J. Nat. Gas Sci. Eng. 77 (2020), pp. 103203. https://doi.org/10.1016/j.jngse.2020.103203

[32] M. Vafaeezadeh, J. Aboudi and M. M. Hashemi, *A novel phenolic ionic liquid for 1.5 molar CO 2 capture: combined experimental and DFT studies*, RSC Adv. 5 (2015), pp. 58005-58009. https://doi.org/10.1039/C5RA09845A

[33] G. Wu, Y. Liu, G. Liu and X. Pang, *The CO2 absorption in flue gas using mixed ionic liquids*, Molecules 25 (2020), pp. 1034. https://doi.org/10.3390/molecules25051034

[34] E. T Ívez, N. Díaz, M. I. Menéndez, D. Suárez and R. López, *Quantum chemical calculations of stability constants: study of ligand effects on the relative stability of Pd (II)-peptide complexes*, Theor. Chem. Acc. 128 (2011), pp. 465-475. https://doi.org/10.1007/s00214-010-0862-z